Hindawi
Complexity
Volume 2020, Article ID 4725808, 19 pages
https://doi.org/10.1155/2020/4725808

WILEY | Hindawi

Research Article

Hierarchical Multiobjective Dispatching Strategy for the Microgrid System Using Modified MOEA/D

Xiaofeng Wan, Hai Lian, Xiaohua Ding, Jin Peng, and Yining Wu

School of Information Engineering, Nanchang University, Nanchang 330031, China

Correspondence should be addressed to Xiaofeng Wan; xfwan@ncu.edu.cn

Received 29 July 2020; Revised 26 August 2020; Accepted 13 September 2020; Published 28 September 2020

Academic Editor: Xin Li

The large-scale electric vehicles connected to the microgrid have brought various challenges to the safe and economic operation of the microgrid. In this paper, a hierarchical microgrid dispatching strategy considering the user-side demand is proposed. According to the operation characteristics of each dispatch unit, the strategy divides the microgrid system into two levels: source-load level and source-grid-load level. At the source-load level, priority should be given to the use of the renewable energy output. On the basis of considering the user demand, energy storage, electric vehicles, and dispatchable loads should be utilized to maximize the consumption of the renewable energy and minimize the user's electricity cost. The source-grid-load level can smooth the tie-line power fluctuation through dispatching of the power grid and diesel generators. Furthermore, the study presents a modified MOEA/D algorithm to solve the hierarchical scheduling problem. In the proposed algorithm, a modified Tchebycheff decomposition method is introduced to obtain uniformly distributed solutions. In addition, initialization and replacement strategies are introduced to enhance the convergence and diversity. A wind-photovoltaic-diesel-storage hybrid power system is considered to verify the performance of the proposed dispatching strategy and the modified algorithm. The obtained results are compared with other dispatching approaches, and the comparisons confirm the effectiveness and scientificity of the proposed strategy and algorithm.

1. Introduction

With the shortage of global resources and the aggravation of ecological pollution, countries all over the world begin to take the microgrid as an important supplement for the operation of the main network [1]. As the basis and core problem of the optimal operation of the microgrid system, economic environment dispatching of the microgrid has been concerned by scholars all over the world. On the premise of meeting the power system security constraints, the economic/environmental dispatching (EED) problem needs to make use of the existing technology to reasonably schedule the microsource operation mode and unit output. On the contrary, the core of the EED problem is to minimize environmental pollution and maximize economic benefits in the whole scheduling period [2].

However, reducing the pollution of the environment and improving the economic benefits of the microgrid are two goals that influence and restrict each other. There is no absolute optimal solution to make both optimal at the same time. Therefore, in order to find the optimal solution to the scheduling problem, scholars from various countries have proposed various schemes. Hernandez-Aramburo et al. [3] established a microgrid model with two reciprocating natural gas generators, cogeneration systems, wind turbines, and photovoltaic arrays. Moreover, the system was optimized with minimum fuel consumption as the objective function. Mohamed and Koivo [4] also considered the model with the lowest operation and maintenance cost and the lowest environmental cost. The multiobjective economic environment scheduling problem is transformed into a single-objective optimization problem by using the maximum fuzzy satisfaction degree in [4], which significantly reduces the calculation difficulty. However, because the membership function is mainly based on the practical experience, the reliability of the optimization result may be

somewhat reduced. Farzin et al. [5] used the nondominant sorting genetic algorithm with elite strategy (NSGA-II) to solve the microgrid scheduling problem, where the objective functions are the minimum operation cost and the minimum load reduction index of the microgrid. In [6], an artificial shark optimization (ASO) was proposed to solve the economical operation problem of the MG. By comparing with other heuristic algorithms, the ASO performs relatively better than the existing techniques.

Farzin et al. and Singh and Khan [5, 6] used classic bionic algorithms to solve the dynamic economic environment dispatching problem in the microgrid and achieved better results. However, as a classic bionic algorithm, its related research and application have been more in-depth and extensive, but it also exposes its integrated evolutionary solution strategy, poor optimization ability for complex optimization problems, and weak ability to cover the optimal frontier [7]. In contrast, the MOEA/D algorithm adopts the method of decomposing multiobjective problems into a certain number of single-objective problems [8]. This algorithm represents a new development direction of multiobjective optimization problems. In recent years, it has gradually attracted extensive attention from scholars. Ross et al. [9] proposed a novel multiobjective dynamic economic emission dispatch (DEED) model considering the EVs and uncertainties of wind power. Also, it proposes a two-step dynamic constraint processing strategy for decision variables based on the penalty function, and on this basis, the multiobjective evolutionary algorithm based on decomposition (MOEA/D) algorithm is improved to solve the problem. The MOEA/Dusing the localized penalty-based boundary intersection (LPBI) method was proposed in [10]. The algorithm is demonstrated to outperform its competitors on the hybrid renewable energy system (HRES) model as well as a set of benchmarks.

EVs have the potential for low-carbon development and sustainable development. EVs with renewables to participate in the scheduling can improve the utilization of energy. Therefore, it is necessary to study how to arrange them to participate in grid dispatching. Based on the randomness of the wind energy and electric vehicles, the probability density function of wind speed and the energy storage and travel characteristic model of EVs are established in [11]. The improved MOEA/D problem is used to solve the DEED problem, but the effect of the load demand on the DEED problem is not considered in [11]. Lu et al. [12] established a multiobjective optimization model of the microgrid including EVs, but only small-scale EVs were considered to connect to the grid. Zhao et al. [13] proposed a distribution network with the inn for electric vehicles and photovoltaic arrays, which verified that fragmented energy management could effectively reduce the fluctuation of renewables. However, only one charging pile was considered, and the grid with a large number of electric vehicles was not considered. Li et al. [14] introduced the double-chain structure and dynamic rotation angle adjustment strategy. It proposed an improved quantum genetic algorithm, optimized the EED problem of EVs connected to the microgrid system, and verified the superiority of this improved algorithm compared with other algorithms. Whether it is a single-objective or multiobjective optimization, the objective function of microgrid scheduling is relatively limited. More importantly, the operation characteristics of distributed energy generation and the interests of users are not adequately considered in those dispatching models.

In addition, in order to fully consider the interests of the user side, some scholars have begun to study the dispatchable load in the microgrid system. The model established in [15], based on the time-of-use power price mechanism, considered the overall economic optimization of multiobjective and multi-interest groups within the microgrid. The model provided effective help for the operation of the microgrid system and realized electric power marketing for the demand side by using a variant of the NSGA-II algorithm. Zheng et al. [16] considered a microgrid composed of distributed energy, energy storage, and transferable loads. And it changed users' electricity consumption habits through dispatchable loads. Strbac et al. [17] reported the electricity price of interruptible loads based on the economic dispatching model's existing price. Qiu et al. [18] considered the cost of the interruptible load and proposed a scheduling model with the objective function of power grid economic optimization. The results showed that the model could improve the flexibility of scheduling in [18].

At the same time, there are many studies on hierarchical scheduling of microgrids and electric vehicles, and many scholars begin to consider the generation-side and the user-side demand comprehensively [19]. Liu et al. [20] proposed the hierarchical energy system management strategy, considering the diversity of the load and the demand-side response. In [20], the microgrid system was divided into the user layer and microsource layer and used the NSGA-II to realize coordinated control between distributed energy resources (DER), controllable loads, and energy storages (ES). Wang et al. [21] proposed a two-stage scheduling strategy, combining day-ahead scheduling with real-time scheduling. Thus, the load management center could conduct rolling optimization by tracking the load curve and then giving a clear charge and discharge plan for EVs. Ye et al. [22] presented a hierarchical multistage scheduling scheme for the AC/DC hybrid active distribution network. This two-level model avoids the difficulty of solving multiobjective optimization and can clarify the role of various stakeholders in the system scheduling. However, few studies comprehensively consider the operating characteristics of DER and generation and load integrated optimal dispatching.

Based on the above background and research results, this paper proposes a microgrid hierarchical dispatching strategy containing wind turbines (WTs), photovoltaic arrays (PVs), diesel generators (DGs), schedulable loads, and EVs. In the microgrid system, the hierarchical strategy gives full consideration to the influence of the user demands on the economic operation. It uses the modified MOEA/D algorithm to solve the problem. In the proposed strategy, according to the operation characteristics of each dispatch unit, the system is divided into the source-load level and the source-gird-load level. At the source-load level, the dispatchable load and the vehicle-to-grid (V2G) model of

electric vehicles are established to maximize the consumption of the renewable energy. Thus, it can achieve peak load cutting of the system load curve and maximize the user's interests. In dispatching of the source-gird-load level, the output of the DGs and the power of connection lines of the main grid are taken as the decision variables. The objectives of the level are to reduce the overall operation cost and power fluctuation between the microgrid and the main grid. On the premise of meeting the grid energy constraint, the overall optimization of the system side and the user side is realized.

The main result of this paper has the following three points: first, it adopts a hierarchical scheduling strategy. Based on the operation characteristics of each dispatch unit, the strategy divides the microgrid system into two levels: source-load level and source-grid-load level. Furthermore, it proves the scientific nature and effectiveness of the dispatching strategy in the simulation. Second, this paper improves the MOEA/D algorithm for solving the multiobjective problem. A modified Tchebycheff decomposition method is introduced as the decomposition approach in order to obtain uniformly distributed Pareto solutions. And this paper proposes a strategy of initializing the primary population based on the constraint violation value. In addition, a replacement strategy based on the maximum fitness value improvement is also integrated. In the end, it proves that hierarchical scheduling is more capable of coordinating the interests of all stakeholders than conventional scheduling strategies. And through the final comparison experiment, it can be indicated that the participation of schedulable load can effectively improve user satisfaction and reduce load variance.

The rest of this paper is organized as follows. Section 2 introduces the hierarchical dispatching strategy and details of the dispatching processes of the source-load level and the source-grid-load level, respectively. In Section 3, it outlines the mathematical models of EVs and dispatchable load, and on this basis, the microgrid hierarchical dispatching model is established. Section 4 describes the modified MOEA/D algorithm in detail and gives the pseudo-code of the improved part. Section 5 realizes the simulation of the scheduling model in Matlab and compares it with other scheduling strategies and the original algorithm, respectively. The conclusion is drawn in Section 6.

2. The Hierarchical Dispatching Strategy of the Microgrid

The microgrid system with controllable loads, EVs, WTs, PVs, DGs, and ES is shown in Figure 1. In order to solve the economic optimization problem of this complex microgrid system, this section proposes a hierarchical scheduling strategy considering the interests of multiple stakeholders and the characteristics of distributed power supply. According to the operation characteristics of each dispatch unit, the strategy divides the microgrid system into two levels, source-load level and source-grid-load level, based on the coordinated and optimized operation of the source-grid-load system.

2.1. Source-Load Level. The purpose of source-load level dispatching is to reduce the peak-valley difference of the total loads. The strategy of the level takes into account the demand response of the user side and guides users to change the way of electricity consumption from the perspective of the electricity market such as electricity price. The consumption of renewable energy can be realized through source-load level dispatching, which makes the load curve closer to the renewable output curve. More importantly, it can well mobilize the enthusiasm of users to participate in grid dispatching, thus improving the reliability and stability of the grid. The dispatching objects of the source-load stage are EVs, ES, and controllable loads.

EVs have dual characteristics of load and onboard energy storage. Reasonable charging and discharging of electric vehicles can effectively achieve peak-load shifting. Since electric vehicles not only need to satisfy users' travel needs but also need to participate in grid dispatching, this paper divides electric vehicles into two categories: one is subjected to users' driving habits, and the other is entirely subjected to the microgrid management, which is fully dispatchable [23]. The probabilistic travel model of EVs, managed by orderly charging and discharging, is subjected to users' driving habits. Its output curve is obtained by the Monte Carlo simulation algorithm [24]. The fully dispatchable EVs can reduce the peak and valley differences of the load, and energy storage cooperates with dispatchable EVs to smooth the load's peak-valley difference.

On the user side, the load can be divided into dispatchable load and undispatchable load [20], in which the dispatchable load can be divided into transferable load and interruptible load. Undispatchable load cannot be interrupted in the optimization process; otherwise, it will cause severe economic loss and social harm. The interruptible load is the lowest among all loads. When the power supply of the system cannot meet all load demands, the load can be interrupted for a short period of time. At this time, corresponding power failure compensation will be provided to the user side [18]. The total electric quantity of the transferable load in the dispatching period is a certain amount. On the premise of not exceeding the maximum allowable transfer electric quantity, the start-up time of the transferable load can be delayed or advanced, such as washing machines and charging equipment in the household load. Therefore, scheduling of the transferable load is an important measure in the microgrid optimal scheduling. It can not only cut the peak and fill the valley and absorb extra renewable energy but also realize the economic operation of the microgrid [16]. The dispatchable load studied in this paper is the transferable load.

The multiobjective optimization algorithm obtains the Pareto optimal solution set with minimum user cost and minimum system net load variance. Using the method of fuzzy membership degree [7], the compromise solution is selected in the Pareto solution set for analysis, and the output curve of each scheduling unit of the solution is substituted into the next step.

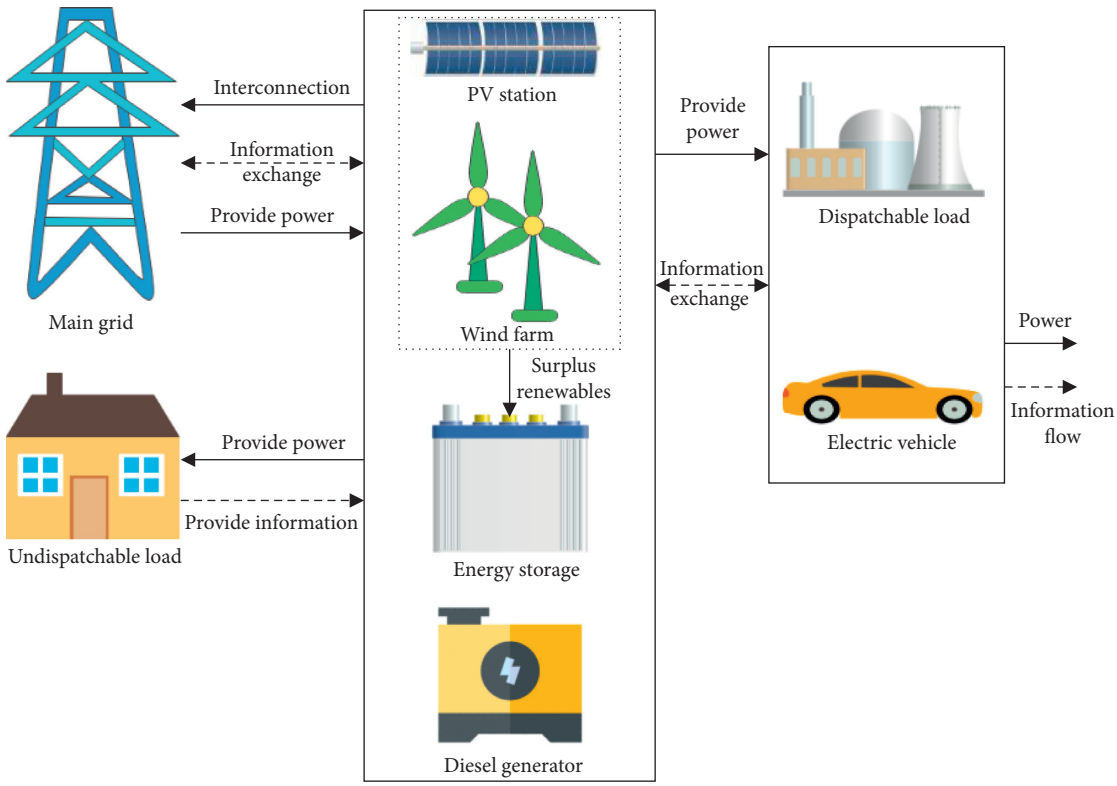

Figure 1: WT-PV-ES-DG-EV hybrid power system with the dispatchable load.

2.2. Source-Grid-Load Level. The net load from the first level is absorbed at the source-grid-load level by the diesel generators and connection lines of the main grid, while the surplus renewable energy is sold to the main grid to gain benefits. The dispatching object of this level is the output of a large power grid and diesel generators. The second dispatching stage's main purpose is to reduce the overall operation cost of the microgrid, as well as the power fluctuation of the connection lines of the grid. The objective function is to minimize the operation cost and the power fluctuation between the microgrid and the main grid. The ramp-rate constraint is adopted for the DGs. And the output upper and lower limits and power balance constraints of the generators should be satisfied at the same time. The net load of the microgrid obtained in the first step is substituted at this level, and the MOEA/D algorithm is used again to obtain the optimal Pareto frontier distribution of the system. After calculation, the compromise optimal solution is selected to discuss the results.

3. Mathematical Model and Characteristic Analysis of the Microgrid

According to the scheduling policy's description, scheduling of the microgrid system is divided into two levels: source-load level and source-grid-load level. This section will carry out mathematical modeling to the EVs and the dispatchable load and establish the corresponding objective function at each level of the system. In order to ensure safe and reliable operation of the system, the last part of this section will systematically introduce the constraints of microgrid scheduling.

3.1. Electric Vehicle Modeling

3.1.1. Probabilistic Model of Electric Vehicle Travel. The probability density functions (PDFs) of the EV's departure and return journey were obtained by fitting the statistical data in [25]. The return trip time of the last trip of electric vehicles satisfies the normal distribution $t_0 \sim N(\mu_t, \sigma_t^2)$, and the PDF is as follows:

$$f_t(x) = \begin{cases} \dfrac{1}{\sigma_t\sqrt{2\pi}} \exp\left(-\dfrac{(x-\mu_t)^2}{2\sigma_t^2}\right), & \mu_t - 12 < x < 24, \\ \dfrac{1}{\sigma_t\sqrt{2\pi}} \exp\left(-\dfrac{(x-(\mu_t-24))^2}{2\sigma_t^2}\right), & 0 < x < \mu_t - 12, \end{cases} \tag{1}$$

where the expectation μ_t is 17.6 and variance σ_t is 3.4.

Driving distance S approximately obeys lognormal distribution $S \sim \log N(\mu_s, \sigma_s^2)$. The PDF is as follows:

$$f_s(x) = \left(\frac{1}{x}\right)\left(\frac{1}{\sigma_s\sqrt{2\pi}}\right)\exp\left(-\frac{(\ln x - \mu_s)^2}{2\sigma_s^2}\right), \tag{2}$$

where the expectation μ_s is 3.2 and the standard deviation σ_s is 0.88.

The daily energy consumption of the electric vehicle can be obtained from the daily driving distance, so as to obtain

the charged state when the battery of the electric vehicle enters the network:

$$S_{\mathrm{OC,EC}} = \left(1 - \frac{\mathrm{SW}_{100}}{100C}\right) \times 100\%, \tag{3}$$

where $S_{\mathrm{OC,EC}}$ is the state of charge (SOC) when entering the network, W_{100} is the power consumption of 100 kilometers, and C is the total capacity of the battery.

$T_{\mathrm{all-disc}}$ is the total discharge duration required to discharge the electric vehicle to the lower limit of the state of charge when it is fully charged:

$$T_{\mathrm{all-disc}} = \frac{\left(S_{\mathrm{OC,max}} - S_{\mathrm{OC,min}}\right)\mathrm{C}}{P_{\mathrm{disc}}}, \tag{4}$$

where $S_{\mathrm{OC,max}}$ and $S_{\mathrm{OC,min}}$ are the upper and lower limits of the charged state of the battery, respectively, and P_{disc} is the discharge power of the EV.

The actual discharge duration T_{disc} is

$$T_{\mathrm{disc}} = T_{\mathrm{all-disc}} - \left(\frac{SW_{100}}{100P_{\mathrm{disc}}}\right). \tag{5}$$

The discharge time $T_{\mathrm{start-disc}}$ is obtained from the comparison between the last return time and the starting time of the morning and evening peak of the original load in the microgrid. The end time of discharge $T_{\mathrm{end-disc}}$ is determined by the beginning time of discharge $T_{\mathrm{start-disc}}$ and the duration of discharge T_{disc}. The upper limit of $T_{\mathrm{end-disc}}$ is 12:00 p.m. Due to the limitation of the discharge time, some EVs have not completely discharged their electricity. Therefore, the initial state of charge at the beginning of charging varies with the discharge condition, and the initial state of charge is only determined by the above discharge condition.

The charging load P_{EV} required by a single electric vehicle is the total energy consumed in a day:

$$P_{\mathrm{EV}} = \left(\frac{\mathrm{SW}_{100}}{100}\right) + P_{\mathrm{disc}}\left(T_{\mathrm{end-disc}} - T_{\mathrm{start-disc}}\right). \tag{6}$$

Since the charging time of each EV is independent, the corresponding parameters of each EV can be obtained by random tests. According to the obtained charging and discharging initial time and the maximum discharge power by the Monte Carlo method, the charging time $T_{\mathrm{char}}(i)$ and discharging time $T_{\mathrm{dischar}}(i)$ of the i-th EV and the daily charging and discharging load $E_{\mathrm{ev}}(t)$ of each EV at time t are decided.

3.1.2. Dispatchable Electric Vehicle Modeling. Large-scale EV which are dispatched directly in the microgrid system will produce "dimension disaster." The area of electric cars is gathered by agents in this paper, equivalent to large aggregate "virtual electric vehicles." Then, through the system scheduling mechanism, all the aggregates are dispatched to alleviate the pressure on the system side [26]. The following part mainly focuses on the scheduling problem of system-side aggregates.

In order to meet the travel characteristics and energy storage characteristics of electric vehicles, this paper makes the following assumptions about dispatchable EVs:

(1) The SOC of electric vehicles is 100% when they leave home every morning

(2) Electric vehicles can drive to and from work within an hour starting at 7 o'clock and 17 o'clock and can flexibly participate in grid dispatching during the rest of the time

The minimum SOC limit and rated charge and discharge power of the vehicle battery in the dispatching cycle are set at 20% of the rated value. And the charging and discharge efficiency is set at 0.85. The total driving distance of each EV in one dispatching period is 50 km. Taking into account the V2G behavior of electric vehicles and considering the energy consumption to meet users' driving needs, the remaining electric quantity S_t of electric vehicles in time t can be obtained [27]:

$$S_t = S_{t-1} + \eta_C P_{\mathrm{Ch},t}\Delta T - \left(\frac{1}{\eta_D}\right)P_{\mathrm{Dch},t}\Delta T - S_{\mathrm{Trip},t}, \tag{7}$$

where η_C and η_D are the charging and discharging efficiency, ΔT is the scheduling interval, and $S_{\mathrm{Trip},t}$ is the energy consumed by the electric vehicle in the process of driving in time period t:

$$S_{\mathrm{Trip},t} = \Delta S \times L, \tag{8}$$

where ΔS presents the average power consumption per unit distance and L is the driving distance.

In order to ensure battery's life and operation safety, its remaining capacity S_t must be limited within a certain range, that is,

$$S_{\min} \le S_t \le S_{\max}, \tag{9}$$

where $S_{\max}$ and $S_{\min}$ are the upper and lower limits of battery power.

The charging and discharging power of an electric vehicle have a certain safety constraint and cannot exceed its rated charging and discharging power as follows:

$$\begin{cases} P_{\mathrm{Ch},t} \le P_{\mathrm{NCh}}, \\ P_{\mathrm{Dch},t} \le P_{\mathrm{NDch}}, \end{cases} \tag{10}$$

where P_{NCh} and P_{NDch} present the rated charging and discharging power of an electric vehicle.

The most important function of electric vehicles is to meet the vehicle owners' travel needs. Since too many charge and discharge cycles will damage the battery life, this paper sets that only one charge and discharge cycle is completed in each scheduling cycle. The vehicle owners' travel needs are constrained as follows:

$$\sum_{t=1}^{T} S_{\mathrm{Trip},t} = \sum_{t=1}^{T} \eta_C P_{\mathrm{Ch},t}\Delta T - \sum_{t=1}^{T} \frac{1}{\eta_D} P_{\mathrm{DCh},t}\Delta T. \tag{11}$$

3.2. Schedulable Load Modeling. Dispatching of the transferable load is an important measure in optimal dispatching of the microgrid. It can also realize peak-load shifting optimization and the absorption of renewable energy, as well as the optimal economic operation of the microgrid. In this paper, the load of the microgrid system is composed of the undispatchable load and transferable load. The load model is as follows [28]:

$$P_L = P_{L,\mathrm{im}} + P_{L,\mathrm{tr}}, \tag{12}$$

where P_L, $P_{L,\mathrm{im}}$, and $P_{L,\mathrm{tr}}$ are, respectively, the total load power of the system, the undispatchable load power, and the transferable load power.

Transferable loads can be transferred from one time period to another, but the total power of transferable loads remains the same in one scheduling period T:

$$P_{L,\mathrm{tr}} = \sum_{t=1}^{T} P_{L,\mathrm{tr}}(t), \tag{13}$$

where $P_{L,\mathrm{tr}}(t)$ is the demand of the transferable load in time period t.

In addition, transferable load shall be transferred within the load power range:

$$P_{L,\mathrm{tr}}^{\min}(t) \le P_{L,\mathrm{tr}}(t) \le P_{L,\mathrm{tr}}^{\max}(t), \tag{14}$$

where $P_{L,\mathrm{tr}}^{\max}(t)$ and $P_{L,\mathrm{tr}}^{\min}(t)$, respectively, represent the upper and lower limits of the power consumption of the transferable load in time t.

3.3. Objective Functions. In this paper, we study the economic scheduling problem of the WT-PV-DG-ES microgrid system, which takes into account V2G and the dispatchable load. Economic scheduling, as a complex multiobjective optimization problem, is worth considering not only the operation cost but also the environmental protection, user satisfaction, and load peak-valley difference. On the one hand, dispatching of the source-load level is to improve the satisfaction of the user's electricity expenditure; on the other hand, it is to realize the absorption of renewable energy and make the load curve fit the renewable energy output as much as possible [21]. The objective functions of the source-grid-load level are the power fluctuation of the tie line between the main grid and the microgrid and the comprehensive operation cost of the system. The objective functions of the optimization model will be established in the following.

3.3.1. User-Side Cost and Load Variance. In the first stage of dispatching, the user cost mainly refers to the user electricity charge C_{load} and the discharge subsidy C_{dis} of V2G:

$$\begin{aligned} f_{\mathrm{user}} &= C_{\mathrm{load}} - C_{\mathrm{dis}}, \\ C_{\mathrm{load}} &= \sum_{t=1}^{T}\left(P_{L,\mathrm{im}}(t) + P_{L,tr}(t) + P_{\mathrm{ev,ch}}(t)\right)p_L(t), \\ C_{\mathrm{dis}} &= \sum_{t=1}^{T} P_{\mathrm{ev,dis}}(t)\,p_{\mathrm{ev}}, \end{aligned} \tag{15}$$

where T is the number of scheduling time periods. Scheduling of the day studied in this paper is 24 hours; $P_{\mathrm{ev,ch}}(t)$ and $P_{\mathrm{ev,dis}}(t)$ are the charging power and discharging power of the EV in time period t, both of which are positive; p_{ev} is the uniform discharge subsidy of the microgrid system to the electric vehicle; and $p_L(t)$ is the TOU (time-of-use) price in t period.

In order to alleviate the impact of the wind turbine and photovoltaic grid connection on the power grid and reduce the fluctuation of the load, the objective function was established by taking the minimum load variance f_{var} of grid connection as the optimization objective [29]:

$$\begin{aligned} f_{\mathrm{var}} &= \left(\frac{1}{T}\right)\sum_{t=1}^{T}\left(P_L(t) + P_{ES}(t) + P_{ev,ch}(t) - P_{ev,dis}(t) - P_{new} - P_{av}\right)^2, \\ P_{\mathrm{av}} &= \sum_{t=1}^{T}\frac{\left(P_L(t) + P_{ES}(t) + P_{ev,ch}(t) - P_{ev,dis}(t) - P_{new}\right)}{24}, \end{aligned} \tag{16}$$

where $P_{\mathrm{ES}}(t)$, P_{new}, and P_{av}, respectively, represent the output of the ES in time period t, the predicted renewable energy output power, and the average load in the dispatching period.

3.3.2. Integrated Operation Cost and Power Fluctuation. At the second-level dispatching, the scheduling objects are the power grid and DGs. It aims to reduce the comprehensive operation cost on the system side and improve the safety and reliability of the microgrid system, which is reflected by the power fluctuation of connection lines of the main grid. Therefore, the objective function is the minimum integrated operation cost $f_{\cos t}$ of diesel generators and the power grid [30] and the power fluctuation f_{flu} of the tie lines.

As the problem of air pollution becomes more and more serious, more and more countries and regions begin to consider environmental protection. However, conventional thermal power units will produce greenhouse gases and air pollutants in the process of power generation, such as SO_x and NO_x [6]. Therefore, it is very necessary to reduce the emission of air pollutants caused by thermal power units. The comprehensive operation cost $f_{\cos t}$ refers to the comprehensive operation cost of DGs $C_{\mathrm{de},\cos t}$ and the power grid $C_{\mathrm{grid,cost}}$. The operating cost of DGs includes operating and maintenance cost $C_{\mathrm{de,om}}$, fuel cost $C_{\mathrm{de,fuel}}$, and environmental governance cost $C_{\mathrm{de,en}}$ [7]:

$$\begin{aligned} f_{\cos t} &= C_{\mathrm{de},\cos t} + C_{\mathrm{grid},\cos t}, \\ C_{\mathrm{de},\cos t} &= C_{\mathrm{de,om}} + C_{\mathrm{de,fuel}} + C_{\mathrm{de,en}}, \\ C_{\mathrm{de,om}} &= \sum_{t=1}^{T} K_{\mathrm{om,de}} P_{\mathrm{de}}(t), \\ C_{\mathrm{de,fuel}} &= \sum_{t=1}^{T}\left(a + bP_{\mathrm{de}}(t) + c\left(P_{\mathrm{de}}(t)\right)^2\right), \\ C_{\mathrm{de,en}} &= \sum_{t=1}^{T}\sum_{k=1}^{K}\left(C_k\gamma_{\mathrm{de},k}\right)P_{\mathrm{de}}(t), \end{aligned} \tag{17}$$

where $K_{om,de}$ is the running maintenance coefficient of the diesel engine; a, b, and c are the fuel coefficients of the diesel engine; C_k is the treatment of category k pollutants; and $\gamma_{de,k}$ is the emission of class k pollutants generated by DG operation.

The operating cost $C_{grid,cost}$ of the main grid connection lines includes the electricity transaction cost $C_{grid,price}$ between the main grid and the microgrid and the environmental governance cost $C_{grid,en}$ generated during operation:

$$\begin{aligned} C_{grid,cost} &= C_{grid,price} + C_{grid,en}, \\ C_{grid,price} &= \sum_{t=1}^{T} p_L(t) P_{grid}(t), \\ C_{grid,en} &= \sum_{t=1}^{T} \sum_{k=1}^{K} \left(C_k \gamma_{grid,k}\right) \left| P_{grid}(t) \right|, \end{aligned} \tag{18}$$

where C_k presents the treatment of category k pollutants; $\gamma_{grid,k}$ is the emission of class k pollutants generated by the grid; and $P_{grid}(t)$ is the tie-line power of the main network at time t, whose value is positive, which means that the microgrid buys electricity from the main grid, and negative means that the microgrid sells electricity to the main grid. The expression of power fluctuation f_{flu} of the connection lines is as follows [31]:

$$f_{flu} = \sum_{t=1}^{T-1} \left| P_{grid}(t+1) - P_{grid}(t) \right|. \tag{19}$$

3.4. System Constraints. In order to ensure normal and safe operation of the system, the following general constraints are required [27].

3.4.1. System Equality Constraint. The power balance constraint is expressed in the form of equality constraint, which represents the unit output's satisfaction with the load in each dispatching period:

$$P_{grid}(t) + P_{new}(t) + P_{de}(t) = P_L(t) + P_{ES}(t) + P_{EV}(t). \tag{20}$$

Interpretation of the equation: $P_{grid}(t)$ represents the power of the main grid connection lines at time t; $P_{new}(t)$ represents the power of the WT and PV predicted at time t; $P_{de}(t)$ is the output of the DGs at time t; $P_L(t)$ is to the net load power of the microgrid system at time t; and $P_{EV}(t)$ and $P_{ES}(t)$, respectively, represent the output state of the EV and ES unit at time t; the positive value represents charging, and the negative value represents discharge. The units of the above parameters are kw·h.

3.4.2. Upper and Lower Bound Constraints.

$$P_{Gi}^{min} \le P_i(t) \le P_{Gi}^{max}, \tag{21}$$

where P_{Gi}^{min} and P_{Gi}^{max} represent the lower and upper limits of power per unit time of generator i, respectively.

3.4.3. Ramp-Rate Constraints. The ramp-rate constraints are the unit lift (drop) power capacity within the unit scheduling period:

$$\begin{aligned} P_i(t) - P_i(t-1) - U_{Ri}\Delta T \le 0, \\ P_i(t-1) - P_i(t) - D_{Ri}\Delta T \le 0, \end{aligned} \tag{22}$$

where U_{Ri} and D_{Ri} are the lift and drop ramp rate of generator i, respectively. The object of the ramp-rate constraint is diesel generator.

3.4.4. Energy Storage Constraints. Constraint of the state of charge is given by

$$S_{min} \le S(t) \le S_{max}. \tag{23}$$

Energy storage output limits:

$$P_{ES}^{min} \le P_{ES}(t) \le P_{ES}^{max}, \tag{24}$$

where S_{max}, S_{min}, P_{ES}^{min}, and P_{ES}^{max} represent the upper and lower limits of the charged state and output of the energy storage unit, respectively.

3.4.5. Spinning Reserve Constraint. The configuration of spinning reserve capacity has played a positive role in the actual operation of the power system. Due to the uncertainty and intermittency of the renewable output, it is necessary to have a certain reserve capacity to ensure the safety and reliability of the grid connection [32].

$$\sum_{i=1}^{N} P_{i,max} + P_{wt} + P_{pt} \ge P_{ev,t} + P_{L,t} + S_{R,t}, \tag{25}$$

where $S_{R,t}$ is the spinning reserve capacity requirement of the system at time t.

4. Modified MOEA/D Algorithm

As described in the previous section, the economic scheduling problem of the microgrid is a multiobjective optimization problem. The optimization problem needs to consider complex unit operation and system constraints, some of which are nonlinear and time-coupled equality and inequality constraints. This section will introduce the general framework of the multiobjective optimization problem. In order to solve this problem, this paper adopts the MOEA/D algorithm and improves some shortcomings of the algorithm. The last part gives detailed steps for the modified MOEA/D algorithm.

4.1. Multiobjective Optimization Problem. In general, a multiobjective optimization problem consists of two or more mutually restrictive objectives to be optimized and a series of equality and inequality constraints to be satisfied.

Multiobjective optimization problems are usually expressed in the following forms [30]:

$$\begin{aligned} &\min F = \{f_1(x), f_2(x), f_3(x), \ldots, f_M(x)\}, \\ &\quad x = [x_1, x_2, x_3, \ldots, x_n], \\ &\text{subject to } g_j(x) \geq 0, \quad j = 1, 2, \ldots, G, \\ &h_k(x) = 0, \quad k = 1, 2, \ldots, H, \\ &x_i^{\min} \leq x_i \leq x_i^{\max}, \quad i = 1, 2, \ldots, n. \end{aligned} \tag{26}$$

In this paper, the i-th objective function of the multiobjective optimization problem is represented by $f_i(x)$; x is an n-dimensional decision vector. And G and H represent the number of inequality constraints and equality constraints, respectively. In single-objective optimization problems, the optimal solution is usually unique. However, due to the mutual restriction between different objective functions in multiobjective problems, the optimal solutions of multiobjective optimization usually consist of a solution set. Therefore, in order to solve the multiobjective optimization problem, it is necessary to understand the concepts of Pareto dominance, Pareto optimal, Pareto-optimal set, and Pareto-optimal front [33]. According to these definitions, a multiobjective optimization problem can be treated as finding Pareto-optimal solutions or approaching the Pareto-optimal front [34].

4.2. The Main Framework for the MOEA/D Algorithm. As described in [35], the objective functions of a multiobjective problem are usually contradictory, and generally, there is no one solution in the feasible region that can minimize all the objective functions at the same time. Therefore, the purpose of the multiobjective optimization problem is to find all the nondominant or noninferior solutions. In order to find all nondominant solutions, the MOEA/D algorithm decomposes a multiobjective problem into a series of single-objective subproblems by using the weighted sum approach, the Tchebycheff approach, and the boundary intersection approach [36]. These subproblems then produce offspring through collaborative optimization using an evolutionary algorithm [8]. These subproblems are optimized by referring to information about their neighborhood problems. The neighborhood relation of subproblems refers to the Euclidean distance based on their aggregation coefficient vectors [8]. Pareto-optimal front of a multiobjective problem can be decomposed into N scalar optimization subproblems in MOEA/D. As described in [34], the above decomposition method transforms the approximate frontier of the multiobjective optimization problem into a series of single-objective optimization problems. Here, we use the Tchebycheff approach to explain the main framework of the MOEA/D algorithm. The j-th single-objective optimization subproblem is expressed as

$$\begin{aligned} g^{\text{te}}\left(x \mid \lambda^j, z\right) &= \max_{1 \leq i \leq m} \left\{\lambda_i^j \left| f_i(x) - z_i^* \right|\right\}. \\ \lambda^j &= \left(\lambda_1^j, \lambda_2^j, \ldots, \lambda_m^j\right)^T. \end{aligned} \tag{27}$$

The MOEA/D algorithm is designed to optimize N problems at the same time rather than to solve multiple problems in one run. In [36], the neighborhood of λ^j is composed of T weight vectors, which are in $\{\lambda^1, \lambda^2, \ldots, \lambda^N\}$, closest to it. Neighborhood weight vectors of λ^j are the neighborhoods of the j-th subproblem. The population is composed of the optimal solution for each subproblem at the moment.

4.3. Improved Tchebycheff Decomposition Method. According to Section 3, the value range and measurement unit of each objective function are different. As a result, each objective function will have a certain weight before being weighted, which may lead to local convergence or failure, to obtain the uniformly distributed Pareto front. For example, the value range of objective 1 is [1500, 1800], and the value range of objective 2 is [30, 50], so the algorithm will focus on the optimization of objective 1 in the process of optimization. Although some articles proposed an improved Tchebycheff approach to reduce the impact of different units and value ranges, a single-target optimization subproblem is as follows [37]:

$$\min g^{\text{tch}}\left(F(x) \mid \omega, z^*\right) = \max_{1 \leq i \leq m} \left\{\frac{f_i(x) - z_i}{\omega_i}\right\}, \tag{28}$$

where m represents m objective functions; $f_i(x)$ and z_i, respectively, represent the i-th objective function value and the ideal value of the objective; and $\omega = (\omega_1, \omega_2, \ldots, \omega_m)^T$ is the weight vector, which satisfies

$$\|\omega\|_1 = \sum_{i=1}^{m} \omega_i = 1. \tag{29}$$

However, when confronted with a complex multiobjective optimization problem, the obtained Pareto front is still not uniform [8]. So here, we propose the modified Tchebycheff approach to overcome the above shortcomings. In the modified Tchebycheff approach, the decomposition of Tchebycheff mentioned above is extended, and a new Tchebycheff decomposition method with a norm constraint on the direction vector is proposed [38]. In this decomposition, each subproblem is constructed based on a direction vector λ, such as (30), which satisfies $\|\lambda^i\|_2 = 1$, rather than the weight vector ω mentioned above. At this point, the representation of each subproblem is shown in (31):

$$\begin{aligned} \lambda^i &= \frac{\omega^i}{\left\|\omega^i\right\|_2}, \quad i = 1, 2, \ldots, N, \\ \lambda^i &= \left(\lambda_1^i, \lambda_2^i, \ldots, \lambda_m^i\right), \quad \left\|\lambda^i\right\|_2 = 1, \end{aligned} \tag{30}$$

$$\min g^{\text{tch}}\left(F(x) \mid \lambda, z^*\right) = \max_{1 \leq i \leq m} \left\{\frac{f_i(x) - z_i}{\lambda_i}\right\}. \tag{31}$$

Based on the modified Tchebycheff decomposition, the particle is in the direction vector corresponding to its subproblem, so the particle distribution is also uniform [38]. Therefore, the improved decomposition method can obtain

a more uniform frontier solution than the original decomposition.

4.4. Initialization Strategy. Obviously, in the microgrid hierarchical dispatching model, there are various high-dimensional nonlinear and time-coupled constraints, which make the feasible solution domain relatively narrow and topologically complex [38]. Therefore, the basic algorithm must be improved according to the characteristics of the problem. And in order to obtain the optimal feasible solution, the effective treatment of the complex constraints of the model is proposed.

Since the process of optimization starts from the initialization of particles, the selection of primary particles is crucial. If the primary particles can be uniformly distributed in the whole space and most of them meet the constraints, the offspring can maintain better diversity in the subsequent process. On the contrary, if all constraints are hard constraints at the beginning of algorithm optimization, such as they are forced to return to the constraint range or constraint boundary when particles do not meet the constraints, it will greatly reduce the diversity of optimization results [38].

Therefore, this paper proposes a strategy of initializing the primary population based on the constraint violation value as outlined in Algorithm 1. First, an initial population P containing N particles is generated according to the given data. And the initial population may not satisfy all the constraint conditions. Secondly, differential evolution is used to generate N offspring, and $2N$ particles are arranged from small to large according to the constraint violations. Then, the first N particles with fewer constraint violations are added to the external file. When comparing the constraint violations of the N-th particle with ξ and the two are equal, it means that the first N particles satisfy all constraints. In order to ensure diversity, ξ is set as a constant close to zero. If the N-th particle constraint violation is lower than ξ, the particles in the external archives are the first-generation population meeting most of the constraints, otherwise back to the second step. Through this optimization, the first-generation particles can enter into the optimization process of the algorithm under the condition that most of the constraints are satisfied. Since the particles are not forced to satisfy all constraints, the diversity is not lost. On the contrary, in the optimization process, the offspring particles just need to make small adjustments to meet the constraints, so the convergence can be achieved at a faster speed.

$$\begin{aligned} g_j(x) &\geq 0, \quad j = 1, 2, \ldots, G, \\ h_k(x) &= 0, \quad k = 1, 2, \ldots, H, \\ \text{violation}(x) &= \sum_{1 \leq j \leq G} \max\left(g_j(x), 0\right) + \sum_{1 \leq k \leq H} \left(h_k(x)\right)^2. \end{aligned} \tag{32}$$

4.5. Replacement Strategy. Population replacement strategy is a key part of MOEAs, which has been studied by many people in recent years [39]. Although most improved population renewal strategies can successfully improve MOEA/D performance, only a part of the subproblem performance can be optimized [40].

This paper adopts a replacement strategy based on the maximum fitness value improvement as outlined in Algorithm 2. Firstly, parameters are initialized that $l = -1$ and MaxFitImp $= -\infty$. Secondly, the difference between the fitness value of offspring particle y and parent particle x^i in each subproblem is obtained. $V_{\text{improvement}}$ represents the value of the improvement of offspring particle y over parent particle x^i in subproblem i. l represents the subproblem of the maximum fitness increase obtained by particle y. Then, if MaxFitImp is greater than zero, the existence of subproblem l is proved. In this subproblem, the fitness value of the parent generation is larger than that of the offspring. It means that offspring y is superior to the parent generation particle, and the corresponding parent particle x^i is replaced by y. Finally, in order to improve the robustness of the algorithm, y is randomly selected to replace a certain number of parent solutions. The pseudo-code of the replacement strategy based on the maximum fitness value improvement is shown as follows:

$$\begin{aligned} V_{\text{improvement}} &= g^{\text{tch}}\left(F\left(x^i\right) \middle| \lambda^i, z\right) - g^{\text{tch}}\left(F\left(y^i\right) \middle| \lambda^i, z\right), \quad i = 1, 2, \ldots, N, \\ l &= \arg\max_{1 \leq i \leq N} \left[g^{\text{tch}}\left(F\left(x^i\right) \middle| \lambda^i, z^*\right) - g^{\text{tch}}\left(F\left(y^i\right) \middle| \lambda^i, z^*\right)\right], \quad i = 1, 2, \ldots, N. \end{aligned} \tag{33}$$

4.6. Best Compromise Solution Based on Fuzzy Decision. After obtaining the Pareto optimal solution set, it is necessary to find the best compromise solution in the final nondominant solution set by decision. In this paper, we use the fuzzy decision function to get a relatively satisfactory final solution in the Pareto front. In order to obtain the most precise judgment for the decision maker, the satisfaction degree of each objective function of the i-th solution can be defined as follows [7]:

$$\mu_{\text{ij}} = \begin{cases} 1, & F_{\text{ij}} \leq \min\left(F_j\right), \\ \dfrac{\max\left(F_j\right) - F_{\text{ij}}}{\max\left(F_j\right) - \min\left(F_j\right)}, & \min\left(F_j\right) \leq F_{ij} \leq \max\left(F_j\right), \\ 0, & \max\left(F_j\right) \leq F_{ij}, \end{cases} \tag{34}$$

Require:
N: population size
EP: external archive, and EP = Ø
V_i: summing all the constraint violations of the i-th solution
Output: population: EP = $\{x^1,\ldots,x^N\}$
Step 1: N particles are generated randomly according to the boundary constraints
Step 2: producing N solutions using the DE operations
Step 3: calculating the overall constraint violations V_i, $i = 1, 2, ..., 2N$
Step 4: sorting the solutions according to the overall constraint violations in the increasing order and selecting the first N number of solutions
Step 5: **If** $V^N > \xi$, **then** set EP = $\{x^1,\ldots,x^N\}$, and return to Step 2
Step 6: output EP = $\{x^1,\ldots,x^N\}$

Algorithm 1: Initialization of the population.

Require:
j: index of the selected subproblem for reproduction.
Neigh$_j$: indices of the neighbor subproblems of the j-th subproblem, Neigh$_j$ = $B_j = \{j_1,\ldots,j_T\}$
N: size of the evolutionary population y: newly generated offspring
z: reference point
λ^i: direction vector x^i: decision vector
F^i: objective function of i-th sub-problem
n_r: maximum number of the replaced parent solutions by one offspring solutions
Output: Population: $\{x^1,\ldots,x^N\}$ objective function values: $\{F^1,\ldots,F^m\}$
Step 1 Initialization:$c = 0$ MaxFitImp = $-\infty l = -1$
Step 2 Find the sub-problem of maximal fitness improvement
For $i = 1$ to N do
$V_{\text{improvement}} = g^{\text{tch}}(F(x^i) \mid \lambda^i, z) - g^{\text{tch}}(F(y) \mid \lambda^i, z)$
If $V_{\text{improvement}} \geq$ MaxFitImp, **then** MaxFitImp = $V_{\text{improvement}}$ and $c = c + 1$
Step 3 Replace a parent solution:
If MaxFitImp > 0, **then** set $x^i = y$, $F(x^i) = \mathrm{F}(y)$ and $c = c + 1$
Step 4 Replace improvable parent solutions randomly:
While $c < n_r$ and Neigh$_j \neq \emptyset$ do
(1) Randomly select an index i from $Neigh_j$
(2) **If** $g^{\text{tch}}(F(x^i) \mid \lambda^i, z) - g^{\text{tch}}(F(x^i) \mid \lambda^i, z) > 0$ then set $x^i = y$, $F^i = F(y)$ and $c = c + 1$
(3) Delete i from Neigh$_j$
End of While

Algorithm 2: Replacing the parent solution.

where μ_{ij} represents the satisfaction degree of the j-th objective function of the i-th solution. The higher the value of μ_{ij} is, the more satisfied the value of the objective function will be; $\min(F_j)$ and $\max(F_j)$ are the minimum and maximum bounds of the j-th objective function, respectively.

For each nondominant solution, the normalized membership function can be expressed as

$$\mu_i = \frac{\sum_{j=1}^{N_{\text{obj}}} \mu_{\text{ij}}}{\sum_{i=1}^{M}\sum_{j=1}^{N_{\text{obj}}} \mu_{\text{ij}}}, \tag{35}$$

where M is the number of nondominant solutions and N_{obj} is the number of objective functions. The larger the value of μ_i, the better the solution, so the maximum value of μ_i is the best compromise.

4.7. Detailed Steps of the Modified MOEA/D Algorithm. The microgrid optimization dispatching problem involves solving control variables and calculating state variables. The control variables of the problem are generator active power outputs. And the state variables are composed of renewable power output and load demand. All the control variables constitute an individual which represents one solution to the microgrid dispatching problem. When using the modified MOEA/D algorithm to solve the multiobjective optimization problem, the detailed steps are shown in Figure 2.

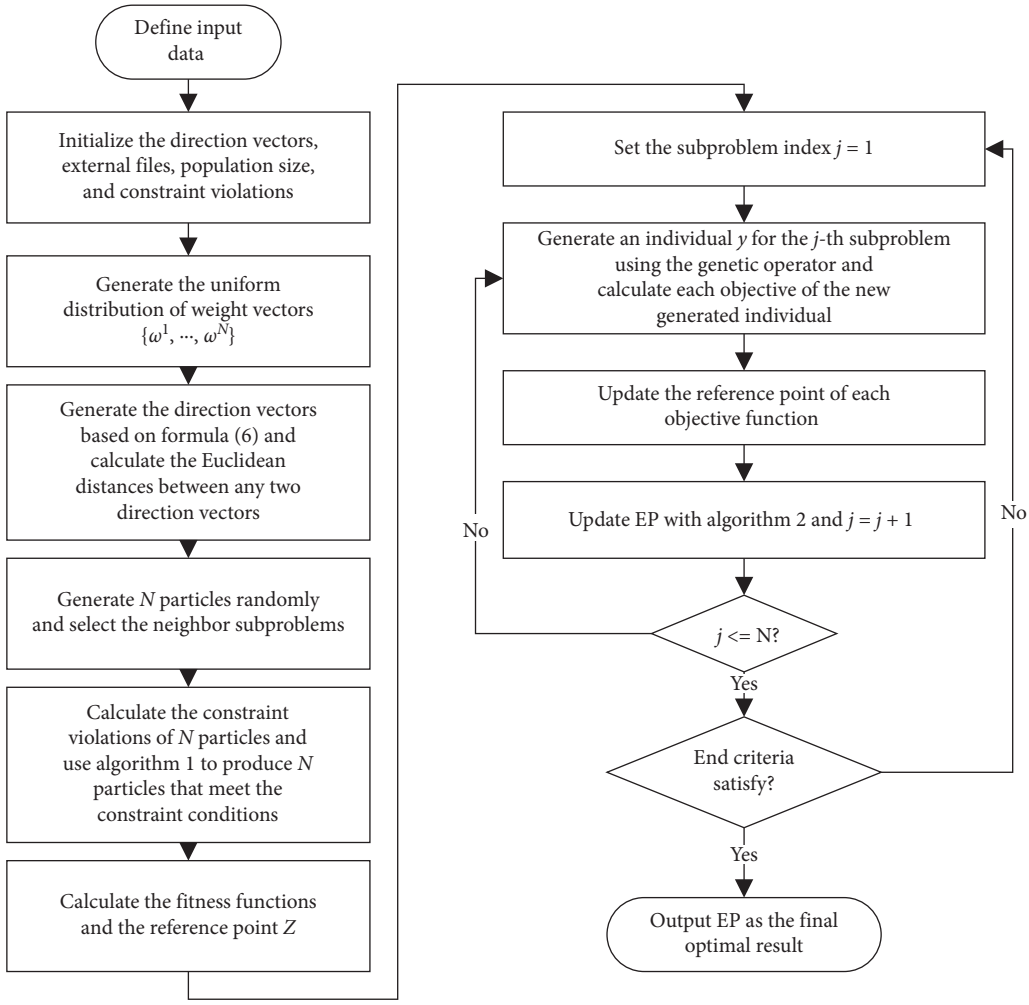

Figure 2: The general main framework of the modified MOEA/D.

5. Simulation Results and Analysis

5.1. Example Parameters. According to the relevant historical data and models, the curve of the renewable energy output and the daily load curve were simulated by the Monte Carlo method [41]. Referring to a real microgrid system in the central region of China, the output of the wind turbine and photovoltaic arrays and the total load are shown in Figure 3, in which the dispatchable load is 10% of the total load. The system contains two diesel generators with a capacity of 0.6 MW and 0.8 MW, respectively, 1 MW lead-acid batteries for energy storage, and 700 EVs with a battery capacity of 24 kw·h. Among them, 400 EVs are subject to user habits, and 300 are fully dispatchable.

In this paper, day-ahead economic dispatching is adopted for the microgrid system, the total dispatching cycle is 24 hours a day, the unit time interval is 1 h, and the electricity price of the main grid adopts TOU price [42]. The electricity price data are shown in Figure 4.

The operating parameters of EVs, ES, DGs, and the power grid are shown in Table 1. And the types of pollutants and the disposing cost are shown in Table 2.

5.2. Obtained Optimal Results

5.2.1. Source-Load Level Dispatching. The Monte Carlo algorithm is used to simulate the travel of 400 EVs. The results and the daily load curve of the system are shown in Figure 5.

As can be seen from the figure, the morning peak load begins to appear in the system at 8:00 a.m., and almost all the EVs finish charging and leave the microgrid system before the morning peak. During the period from 9:00 a.m. to 16:00 p.m., the EVs neither charge nor discharge, that is, they are off the grid. After 17:00 p.m., the EVs return to discharge and participate in system dispatching. And the travel curve is more in line with the user's travel habits. On the contrary, the charging time of EVs is basically from 23:00 p.m. to 8:00 a.m., when the total load is in a low state, and the electricity price is low. Obviously, charging in this period can save charging cost for users. Electric vehicles return to the system after 17:00 p.m. to support peak load demand by discharging. It can alleviate the power shortage in the evening peak and obtain the discharge subsidy. WT, PV, ES, transferable loads, and EVs participate in level dispatching. The simulated traffic data of 400 electric vehicles and the microgrid load are substituted into the mathematical model established above. The objective functions

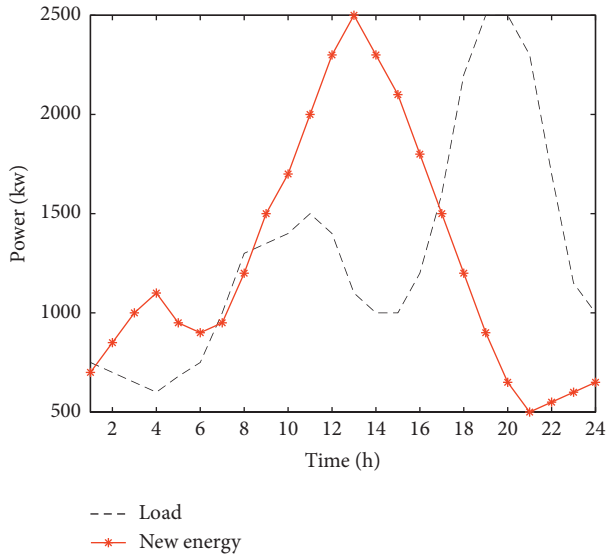

Figure 3: Load curve and renewable energy output curve.

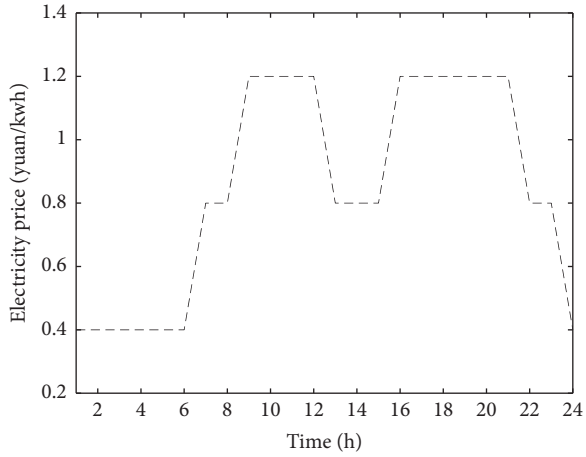

Figure 4: Electric TOU price.

are user cost and load variance in level dispatching. The Pareto front is obtained by using the modified MOEA/D algorithm, as shown in Figure 6.

The fuzzy decision method is used to select (13,732 kw, 25,437 yuan) as the final compromise solution for further analysis. As shown in Figure 7, afterLoad and Load represent the load curves of the transferable load participating in scheduling and not participating in scheduling. And trLoad represents the outpower of the transferable load. It can be seen from the figure that, between 11:00 and 16:00, the electricity price is low, and the power of renewables is large. Thus, most of the transferable loads participate in dispatching in this time period, and the load value of afterLoad is higher than the original load value in this time period. It can be indicated that the original load curve's peak value is greatly reduced when the schedulable load is added.

The curve of netLoad represents the net load of the user side in Figure 8. The netLoad value consists of undispatchable loads, transferable loads, energy storage, and two types of EVs. And the curve of EV is the charging and discharging power of dispatchable EVs. As can be seen from Figure 8, the trend of the EV curve basically follows the output power curve of the renewables. The EVs are driven off-grid from 7:00 a.m. to 8:00 a.m. and from 17:00 p.m. to 18:00 p.m. Then, EVs participate in microgrid scheduling with energy storage in the rest of the time. The output of the energy storage unit also follows the total output of the renewables and the load curve, but the output is not very obvious due to the limitation of its SOC. During the evening peak, EVs discharge along with the energy storage to provide power to the load. When the output of renewable energy is enough to meet the load demand, the energy storage battery and electric vehicle are charged to absorb the redundant renewable energy. At the same time, it can be seen from the figure that the net load curve has been as close to the renewable energy output curve as possible. Thus, it demonstrates that the purpose of maximizing the consumption of renewable energy is achieved. Due to the limitation of the SOC of the energy storage unit, all the surplus renewables have not been absorbed in some periods. The surplus power will be sold to the main grid in the next step.

5.2.2. Source-Grid-Load Level Dispatching. In this stage, the modified MOEA/D algorithm is still used to solve the problem. The objective functions are the minimization of the total operating cost of the system and the power fluctuation of the tie lines. The Pareto front obtained by MOEA/D has been illustrated in Figure 9. It can be seen from the figure that the Pareto front is uniformly distributed. According to the fuzzy decision degree, the compromise optimal solution of the curve is selected, and the results are discussed.

The power outputs of the connection lines and two DGs are shown in Figure 10. If the curve of the grid is negative, it means that the surplus renewables are sold to the main network. The curve of netLoad in the figure consists of the original undispatchable load, the transferable load, the EVs, the ES, and the renewable output. From 7:00 a.m. to 22:00 p.m., renewable energy power is still not consumed after the first step of optimization. Thus, the value of netLoad at this time is less than zero. The redundant renewables are sold to the main network through the connection lines to obtain income for the microgrid side. At this time, the diesel generator stops working, and the power of the connection lines is the same as the netLoad value. When netLoad is positive, the needed power is mainly provided by the main grid due to the low electricity price and the expensive generation cost of the DGs. It can be seen from the figure that the power of tie lines basically fluctuates with the netLoad curve. Two diesel generators are used as the backup supplementary power supply to provide partial power support for the load of the microgrid.

5.3. Comparison of Algorithms. In order to prove the effectiveness of the improved algorithm, this part uses the initial MOEA/D algorithm to solve the hierarchical scheduling problem. We take source-load level scheduling as an example and compare the Pareto solution sets that the two algorithms obtained as follows.

Table 1: Operating parameters.

Operating parameter	Type				
	EV	ES	DG1	DG2	Grid
P_min (kw)	4	200	600	800	1500
P_max (kw)	−4	−200	0	0	−1000
C_min (kw)	—	—	100	150	—
C_max (kw)	—	—	−100	−150	—
Discharge efficiency	0.9	0.9	—	—	—
Charge efficiency	0.9	0.9	—	—	—
S_min (kw)	0.3	0.25	—	—	—
S_max (kw)	0.9	0.95	—	—	—
Operation and maintenance coefficient (yuan/kw)	—	0.104	0.236	0.236	—

Table 2: Pollutant emission factor and disposing cost.

Emission type		CO_2	SO_2	NO_x
Cost (yuan/kg)		0.21	14.824	62.964
Emission	DG	649	0.206	9.89
Coefficient (g/kw·h)	Grid	889	1.8	1.6

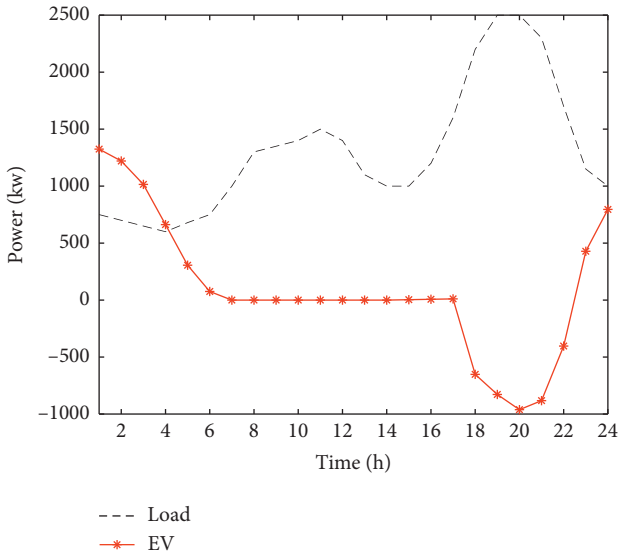

Figure 5: Daily load curve and output of EVs following users' driving habits.

As can be seen in Figure 11, the improved MOEA/D algorithm is closer to the real Pareto frontier than the original algorithm. In order to further explain the performance of the improved algorithm better than the original algorithm, the relationship between the objective functions and the number of iterations is shown in Figure 12.

It can be seen from the figure that although both algorithms eventually converge to the approximate position in the same objective functions, the improved MOEA/D algorithm converges faster than the original algorithm. More importantly, the improved MOEA/D algorithm can eventually reach a smaller value of objective functions. It indicates that the modified MOEA/D algorithm is more effective in this problem.

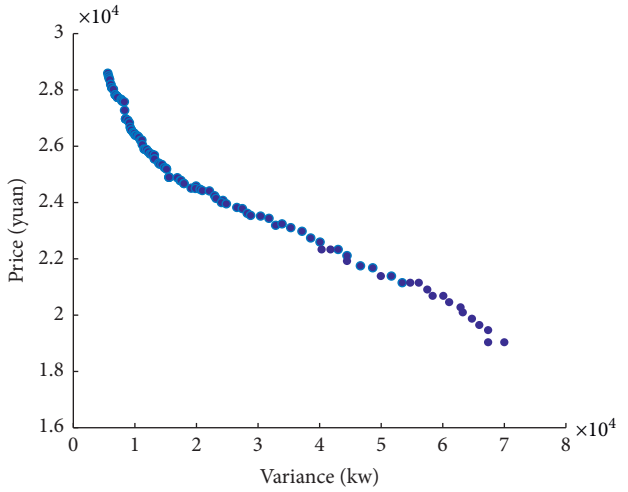

Figure 6: Pareto front of the source-load level.

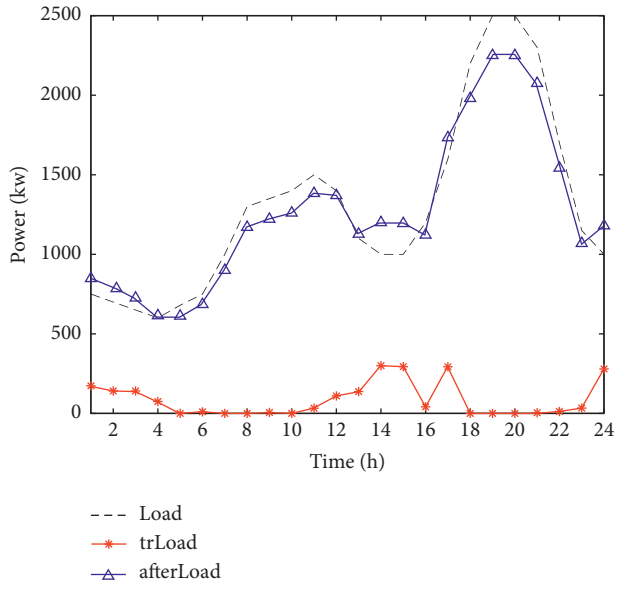

Figure 7: Load curves after dispatching.

5.4. Analysis of Dispatchable Loads. According to Qiu et al. [18], this section establishes the source-load level scheduling strategy excluding the dispatchable load and compares it with

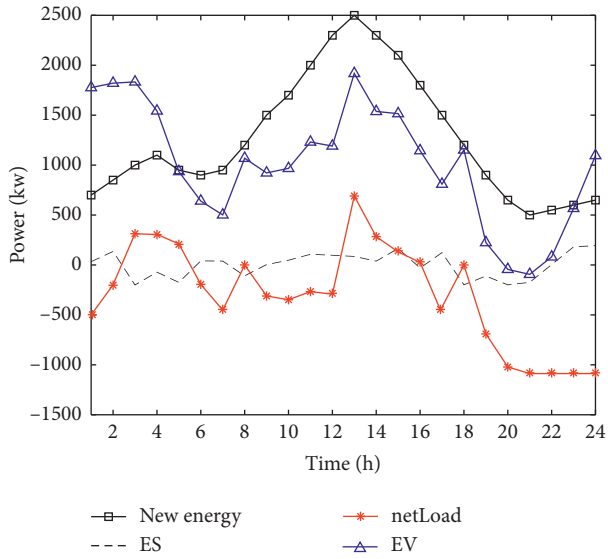

Figure 8: Power output of each unit at the source-load level.

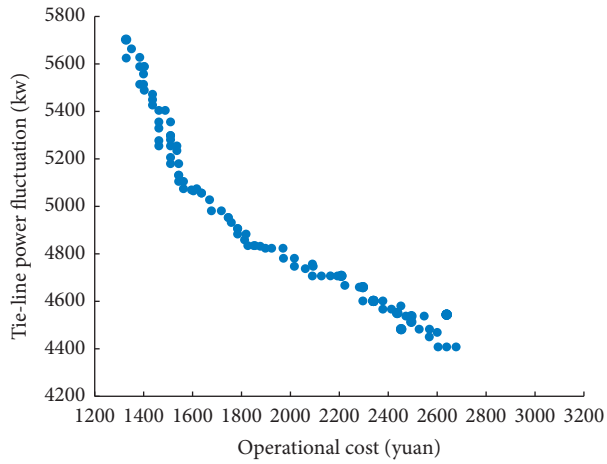

Figure 9: Pareto front of the source-grid-load level.

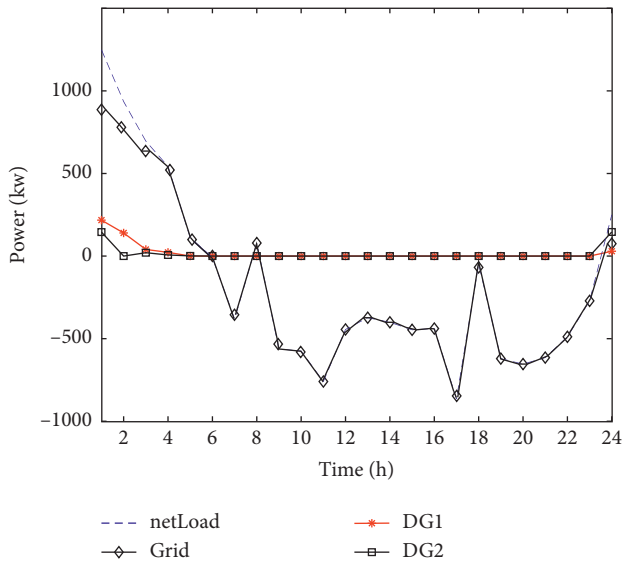

Figure 10: Power output of each unit at the source-grid-load level.

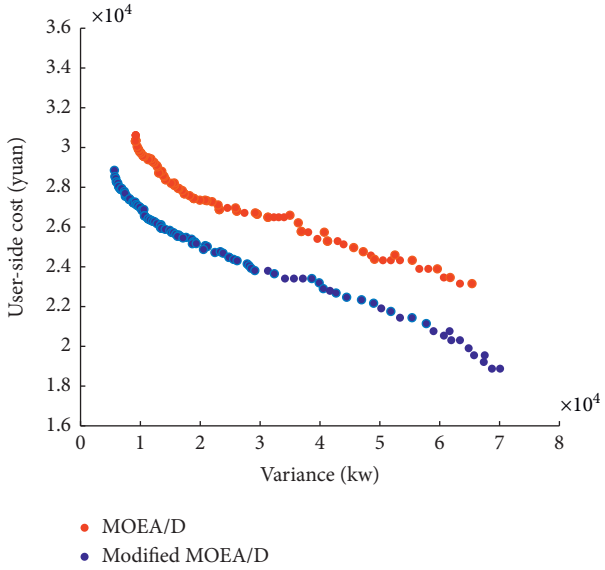

Figure 11: Algorithmic comparison.

the scheduling model proposed in this paper. The strategy of nonconsidering dispatchable loads is adopted in the source-load level, and the curve of netLoad is shown in Figure 13. By comparison with Figure 6, it can be seen that the netLoad curve still follows the output of renewables in Figure 13. However, after considering the schedulable load, the netLoad curve is more consistent with the renewable energy curve in Figure 6, especially in the period from 1:00 to 4:00.

In order to better illustrate the satisfaction of the user side after joining the demand-side response, this section divides user satisfaction into two aspects of comfort and economy:

$$\begin{aligned} U_{\text{com}} &= 1 - \frac{\sum_{t=1}^{24} |\Delta P_t|}{\sum_{t=1}^{24} P_L^{\text{before}}(t)}, \\ U_{\text{eco}} &= 1 - \frac{\sum_{t=1}^{24} p_L(t)\left(P_L^{\text{after}}(t) - P_L^{\text{before}}(t)\right)}{\sum_{t=1}^{24} p_L(t) P_L^{\text{before}}(t)}, \\ U &= U_{\text{com}} U_{\text{eco}}, \end{aligned} \tag{36}$$

where U_{com}, U_{eco}, and U represent the degree of comfort, economy, and comprehensive satisfaction of users, respectively. And $|\Delta P_t|$ is the sum of the absolute value of the electric quantity change in each period before and after the optimization; it is equal to the dispatching load in this paper. $P_L^{\text{before}}(t)$ and $P_L^{\text{after}}(t)$ represent the total load value of t period before and after optimization. The comprehensive satisfaction degree of users is introduced to quantify the satisfaction degree of the scheduling strategy. When the schedulable load is not considered, the user's comfort degree is the largest. At the same time, U_{com} and U_{eco} are all equal to one. The load variance value, user-side cost, and user satisfaction rate of the two strategies are shown in Table 3.

From Table 3, it can be indicated that, due to considering the transferable loads, some of the loads will be shifted to the period with a low price in the proposed strategy. Thus, the user-side cost is smaller than the strategy of nonconsidering

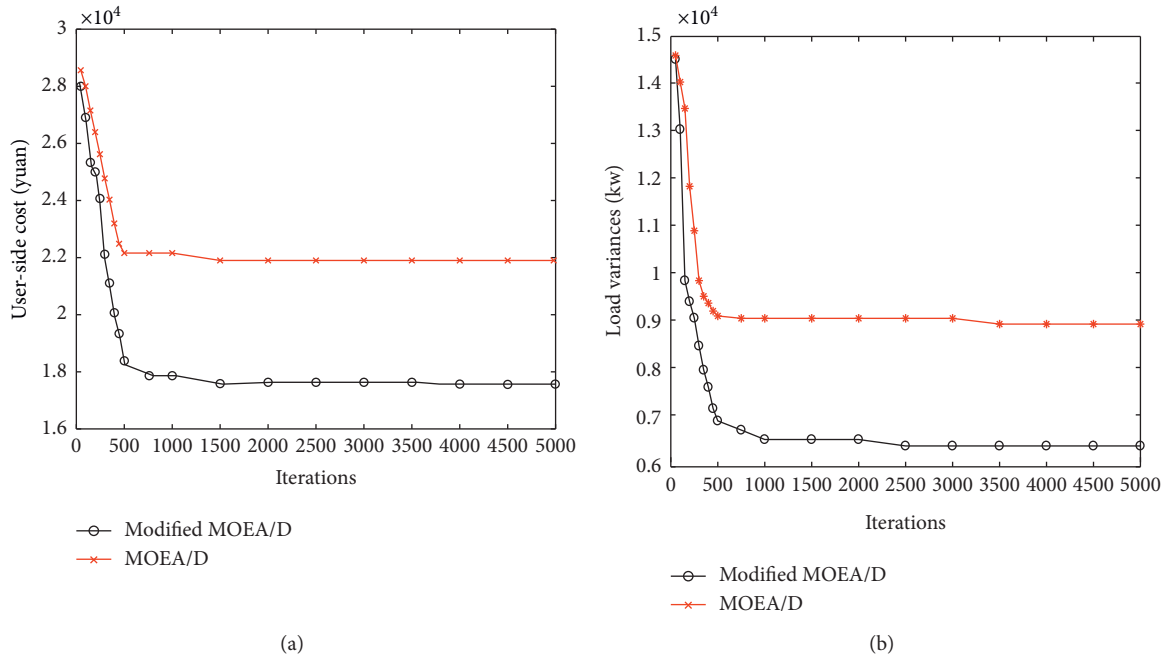

Figure 12: Comparison of convergence. (a) The curve of the value of the user-side cost. (b) The curve of the value of load variances.

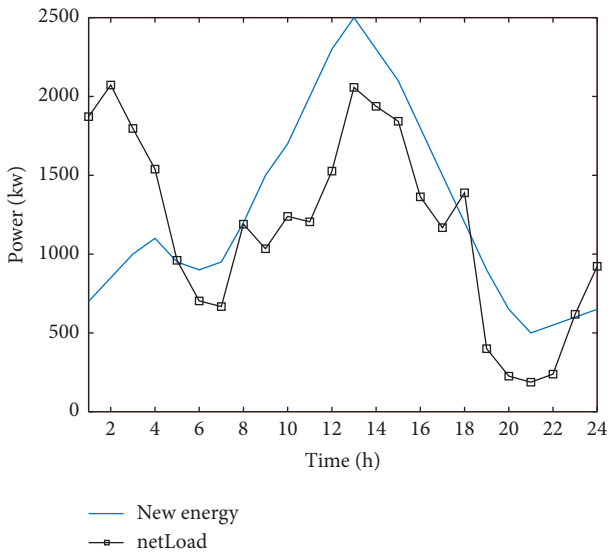

Figure 13: The curve of netLoad and renewables in the strategy without considering the dispatchable load.

dispatchable loads. At the same time, the dispatchable load can improve renewable energy utilization and reduce the load variance. By comparing the user satisfaction degrees, it can be seen that the comfort degree decreased by 11%, but the electricity cost decreased by 16%, and the overall satisfaction increased by 4%.

It can be indicated that the proposed strategy can reduce the impact on users' comfort as much as possible and maximize the economic benefits of users. Therefore, the strategy with dispatchable loads can maximize users' satisfaction, and the transferable loads can greatly optimize the scheduling results in the dispatching process.

5.5. Comparison with the Nonhierarchical Dispatching Strategy. In the microgrid system mentioned above, the dispatching strategy without considering hierarchy is used to solve the optimization problem. For a comprehensive comparison, the nonhierarchical scheduling strategy is divided into nonhierarchical scheduling 1 and nonhierarchical scheduling 2. The objective functions of nonhierarchical scheduling 1 are the lowest user cost and operating cost of the microgrid, while the objective functions of nonhierarchical scheduling 2 are the minimum load variance and the minimum power fluctuation of the connection lines. These two scheduling problems are still multiobjective optimization problems, so the modified MOEA/D algorithm is adjustable to solve them. The operation results of the three scheduling policies are compared, as shown in Table 4.

As can be seen from Table 4, compared with the result of the hierarchical scheduling strategy, the user-side cost and microgrid cost increased by 40% and 10%, respectively, in nonhierarchical strategy 1. In a dispatching period, the load variances of nonhierarchical strategy 2 increased by 21%, and the power fluctuation of the tie lines increased by 32%. It can be drawn that the hierarchical strategy can obtain better optimization results than nonhierarchical strategies in the same objective functions. Besides, the optimization of the other two objectives can be realized in the hierarchical strategy. It can be seen that, in the microgrid system proposed in this paper, the indexes of the hierarchical strategy are better than those of the nonhierarchical strategy. And the result of this comparative experiment proves the comprehensiveness of hierarchical scheduling.

Table 3: Comparison of simulation results of dispatching strategies.

Dispatching strategy	Load variance	User-side cost	U_{com}	U_{eco}	U
Considering dispatchable load	13732	25437	0.89	1.16	1.04
Nonconsidering dispatchable load	19969	27957	1	1	1

Table 4: Comparison of operation results of three dispatching models.

Dispatching strategy	Load variance	User-side cost	Operating cost of the microgrid	Tie-line power fluctuation
Hierarchical strategy	13732	25437	1675	5073
Nonhierarchical strategy 1	30622	27980	2345	9131
Nonhierarchical strategy 2	16616	43752	3786	6696

6. Conclusion

In this paper, a microgrid hierarchical dispatching strategy is proposed. The source-load level strategy considers user-side fees, and load variance, the operation cost of the microgrid, and the power fluctuation of the connection lines are minimized at the source-grid-load level of the system. The modified MOEA/D algorithm is used to solve the optimal dispatching problem. Through analysis and comparison with the result of the final scheduling, the following conclusions can be drawn:

(1) The participation of schedulable load and EVs in microgrid dispatching has a significant effect on peak load clipping and valley filling of the load curve. Moreover, it also improves the utilization rate of renewable generation and the microgrid's income to a certain extent.

(2) By comparing the modified MOEA/D with the original algorithm, it can be found that the replacement strategy based on the maximum value and the initialization strategy based on the constraint violations can effectively improve the convergence speed of the algorithm.

(3) The hierarchical scheduling strategy can fully consider the operation characteristics of the generation units at each level of scheduling. It can not only improve the overall satisfaction of users but also reduce the economic operation cost of the microgrid. Thus, the proposed strategy can realize the win-win situation of user satisfaction, good economy, and high system security.

Abbreviations

Parameters

μ_t: Expectation of t_0
σ_t: Variance of t_0
μ_s: Expectation of S
σ_s: Standard deviation of S
W_{100}: Power consumption of 100 kilometers
C: Total capacity of the EV battery
$S_{OC,max}(S_{OC,min})$: Upper (lower) limit of the SOC
η_C, η_D: Charging and discharging efficiency
ΔT: Scheduling interval
ΔS: Average power consumption per unit distance
$S_{max}(S_{min})$: Upper (lower) limits of battery power
$P_{NCh}(P_{NDch})$: Rated charging (discharging) power of an EV
P_L: Total load power of the system
$P_{L,tr}$: Transferable load power
C_{dis}: Discharge subsidy
T: Number of scheduling time periods
p_{ev}: Uniform discharge subsidy of the microgrid system to the electric vehicle
$K_{om,de}$: Running maintenance coefficient
$U_{Ri}(D_{Ri})$: Lift (drop) ramp rate of generator i
$S_{max}(S_{min})$: Upper (lower) limits of the SOC
$P_{ES}^{min}(P_{ES}^{max})$: Upper (lower) output limits of ES
x: Decision vector
λ: Direction vector
G: Number of inequality constraints
H: Number of equality constraints
m: Objective functions
ω: Weight vector
ξ: A constant close to zero
N: Population size
EP: External archive
y: Offspring particle
z: Reference point
N_{obj}: Number of objective functions
M: Number of nondominant solutions
a, b, c: Fuel coefficients of the diesel engine

Variables

t_0: Return trip time of the last trip of electric vehicles
S: Driving distance
$S_{OC,EC}$: SOC of the EV battery
P_{disc}: Discharge power of the EV
$T_{start-disc}(T_{end-disc})$: Beginning (end) time of EV discharge
T_{disc}: Duration of discharging
P_{EV}: Charging load of the EV
$T_{char}(i)(T_{dischar}(i))$: Charging (discharging) time of the i-th EV

$E_{ev}(t)$: Daily charging and discharging load of each EV at time t
S_t: Remaining electric quantity of an electric vehicle in time t
$S_{\text{Trip},t}$: Energy consumed by the electric vehicle in the process of driving in time period t
L: Driving distance
$P_{L,\text{tr}}^{\max}(t)(P_{L,\text{tr}}^{\min}(t))$: Upper (lower) limits of the power consumption of the transferable load in time t
C_{load}: User electricity charge
$P_{\text{ev,ch}}(t)(P_{\text{ev,dis}}(t))$: Charging (discharging) power of the EV in time period t
p_L: TOU price
f_{var}: Load variance
P_{ES}: Output of the ES
P_{new}: Predicted renewable energy output power
P_{av}: Average load
$f_{\cos t}$: Integrated operation cost of DGs and the power grid
f_{flu}: Power fluctuation of the tie lines
$C_{\text{de, cos}t}$: Comprehensive operation cost of DGs
$C_{\text{grid, cos}t}$: Comprehensive operation cost of the power grid
$C_{\text{de,om}}$: Operating and maintenance cost of DGs
$C_{\text{de,fuel}}$: Fuel cost of DGs
$C_{\text{de,en}}$: Environmental governance cost of DGs
C_k: Treatment of category k pollutants
γ_{de}: Emission of pollutants generated by DGs
$C_{\text{grid,price}}$: Electricity transaction cost
$C_{\text{grid,en}}$: Environmental governance cost
γ_{grid}: Emission of pollutants generated by the grid
P_{grid}: Tie-line power of the main network
P_{de}: Output of the DGs
P_{new}: Power of the WT and PV predicted
P_{ES}: Output state of ES
S_R: Spinning reserve capacity requirement of the system
$f_i(x)$: i-th objective function of the multiobjective optimization problem
z_i: Ideal value of the i-th objective function
V_i: Summing all the constraint violations of the i-th solution
$V_{\text{improvement}}$: Value of the improvement of the offspring particle
l: Subproblem of the maximum fitness
Neigh_j: Indices of the neighbor subproblems of the j-th subproblem
F^j: Objective function of the j-th subproblem
n_r: Maximum number of the replaced parent solutions by one offspring solution
μ_{ij}: Satisfaction degree of the j-th objective function of the i-th solution
U_{com}: Degree of comfort satisfaction of users
U_{eco}: Degree of economy satisfaction of users
U: Degree of comprehensive satisfaction of users
$|\Delta P_t|$: Sum of the absolute value of the electric quantity change in each period
$P_L^{\text{before}}(t)$: Total load value of t period before optimization
$P_L^{\text{after}}(t)$: Total load value of t period after optimization

Acronyms

EED: Economic/environmental dispatching
NSGA-II: Nondominant sorting genetic algorithm with elite strategy
ASO: Artificial shark optimization
MG: Microgrid
DEED: Dynamic economic emission dispatch
MOEA/D: Multiobjective evolutionary algorithm based on decomposition
LPBI: Localized penalty-based boundary intersection
HRES: Hybrid renewable energy system
EV: Electric vehicle
DER: Distributed energy resources
ES: Energy storages
WT: Wind turbine
PV: Photovoltaic arrays
DG: Diesel generator
V2G: Vehicle-to-grid
SOC: State of charge
TOU: Time of use
PDF: Probability density function.

Data Availability

The data used to support the findings of this study are available from the corresponding author upon request.

Conflicts of Interest

The authors declare no conflicts of interest.

Authors' Contributions

X.W., H.L., and X.D. conceived and designed the study; X.W. and H.L. performed the study; X.W., J.P., and Y.W. reviewed and edited the manuscript; and X.W. and H.L. wrote the paper. All authors read and agreed to the published version of the manuscript.

Acknowledgments

This work was supported in part by the National Natural Science Foundation of China (NSFC: 61563034), the International S&T Cooperation Program of China (ISTCP: 2014DFG72240), and Higher School Science and Technology Floor Plan in Jiangxi Province (KJLD14006).

References

[1] R. Bayindir, E. Hossain, and S. Vadi, "The path of the smart grid-the new and improved power grid," in *Proceedings of the International Smart Grid Workshop And Certificate Program (ISGWCP)*, pp. 1–8, Istanbul, 2016.

[2] C. Wei, X. Bai, and T. Kim, "Advanced control and optimization for complex energy systems," *Complexity*, vol. 2020, p. 3, Article ID 5908102, 2020.

[3] C. A. Hernandez-Aramburo, T. C. Green, and N. Mugniot, "Fuel consumption minimization of a microgrid," *IEEE Transactions on Industry Applications*, vol. 41, no. 3, pp. 673–681, 2005.

[4] F. A. Mohamed and H. N. Koivo, "Online management of microgrid with battery storage using multiobjective optimization," in *Proceedings of the International Conference on Power Engineering, Energy and Electrical Drives (POWERENG)*, pp. 231–236, Setubal, Portugal, 2007.

[5] H. Farzin, M. Fotuhi-Firuzabad, and M. Moeini-Aghtaie, "A stochastic multi-objective framework for optimal scheduling of energy storage systems in microgrids," *IEEE Transactions on Smart Grid*, vol. 8, no. 1, pp. 117–127, 2017.

[6] P. Singh and B. Khan, "Smart microgrid energy management using a novel artificial shark optimization," *Complexity*, vol. 2017, Article ID 2158926, 2020.

[7] J. Zhang, Q. Tang, P. Li, D. Deng, and Y. Chen, "A modified MOEA/D approach to the solution of multi-objective optimal power flow problem," *Applied Soft Computing*, vol. 47, pp. 494–514, 2016.

[8] Q. Zhang and H. Li, "MOEA/D: a multiobjective evolutionary algorithm based on decomposition," *IEEE Transactions on Evolutionary Computation*, vol. 11, no. 6, pp. 712–731, 2007.

[9] M. Ross, C. Abbey, F. Bouffard, and G. Joos, "Multiobjective optimization dispatch for microgrids with a high penetration of renewable generation," *IEEE Transactions on Sustainable Energy*, vol. 6, no. 4, pp. 1306–1314, 2015.

[10] M. Ming, R. Wang, Y. Zha et al., "Multi-objective optimization of hybrid renewable energy system using an enhanced multi-objective evolutionary algorithm," *Energies*, vol. 6, 2017.

[11] Y. Zhu, H. Gao, J. Xiao, B. Qu, F. Zhu, and L. Yang, "Dynamic multi-objective dispatch considering wind power and electric vehicles with probabilistic characteristics," *IEEE Access*, vol. 7, pp. 185634–185653, 2019.

[12] X. Lu, K. Zhou, and S. Yang, "Multi-objective optimal dispatch of microgrid containing electric vehicles," *Journal of Cleaner Production*, vol. 165, pp. 1572–1581, 2017.

[13] Z. Zhao, K. Wang, X. Jiang, and X. Wang, "Economic dispatch of distribution network with inn for electric vehicles and photovoltaic," *The Journal of Engineering*, vol. 2019, no. 16, pp. 2864–2868, 2019.

[14] Q. Li, S. Huang, Y. Cheng et al., "Economic optimization of microgrid based on improved quantum genetic algorithm," *Gaoya Dianqi/High Voltage Apparatus*, vol. 54, no. 3, pp. 136–145, 2018.

[15] F. Zhao, J. Yuan, and N. Wang, "Dynamic economic dispatch model of microgrid containing energy storage components based on a variant of NSGA-II algorithm," *Energies*, vol. 12, 2019.

[16] Y. Zheng, S. Li, and R. Tan, "Distributed model predictive control for on-connected microgrid power management," *IEEE Transactions on Control Systems Technology*, vol. 26, no. 3, pp. 1028–1039, 2018.

[17] G. Strbac, E. D. Farmer, and B. J. Cory, "Framework for the incorporation of demand-side in a competitive electricity market," *IEE Proceedings-Generation, Transmission and Distribution*, vol. 143, no. 3, pp. 232–237, 1996.

[18] J. Qiu, J. Zhao, and D. Wang, "Multi-objective generation dispatch considering the trade-off between economy and security," *IET Generation, Transmission & Distribution*, vol. 12, no. 3, pp. 633–642, 2018.

[19] T. U. Solanke and V. K. Ramachandaramurthy, "A review of strategic charging discharging control of grid connected electric vehicles," *Journal of Energy Storage*, vol. 28, 2020.

[20] H. Liu, T. L. Pan, and Z. L. Hao, "Hierarchical optimal dispatching strategy for microgrid system considering user-side resources," in *Proceedings of the 13th IEEE Conference on Industrial Electronics and Applications (ICIEA)*, pp. 1637–1642, Wuhan, China, 2018.

[21] X. Wang, C. Sun, R. Wang, and T. Wei, "Two-stage optimal scheduling strategy for large-scale electric vehicles," *IEEE Access*, vol. 8, pp. 13821–13832, 2020.

[22] C. Ye, S. Miao, Y. Li et al., "Hierarchical scheduling scheme for AC/DC hybrid active distribution network based on multi-stakeholders," *Energies*, vol. 11, 2018.

[23] L. T. Al-Bahrani, B. Horan, and M. Seyedmahmoudian, "Dynamic economic emission dispatch with load demand management for the load demand of electric vehicles during crest shaving and valley filling in smart cities environment," *Energy*, vol. 195, 2020.

[24] Y. Zhou, Z. Li, and X. Wu, "The multiobjective based large-scale electric vehicle charging behaviours analysis," *Complexity*, vol. 2018, p. 16, Article ID 1968435, 2018.

[25] R. Ewing and O. Clemente, "Validation of measures," *Measuring Urban Design*, vol. 46, pp. 83–98, 2013.

[26] Z. A. Arfeen, A. B. Khairuddin, A. Munir et al., "En route of electric vehicles with the vehicle to grid technique in distribution networks Status and technological review," *Energy Storage*, vol. 2, no. 2, 2019.

[27] H. Jiang, S. Ning, and Q. Ge, "Multi-objective optimal dispatching of microgrid with large-scale electric vehicles," *IEEE Access*, vol. 7, pp. 145880–145888, 2019.

[28] P. Palensky and D. Dietrich, "Demand side management: demand response, intelligent energy systems, and smart loads," *IEEE Transactions on Industrial Informatics*, vol. 7, no. 3, pp. 381–388, 2011.

[29] M. Hashim and J. Yong, "Coordinated vehicle-to-grid scheduling to minimize grid load variance," in *Proceedings of the International Conference on Electrical, Electronics and Computer Engineering (UPCON)*, pp. 1–6, Singapore, 2019.

[30] B. Y. Qu, J. J. Liang, Y. S. Zhu, Z. Y. Wang, and P. N. Suganthan, "Economic emission dispatch problems with stochastic wind power using summation based multi-objective evolutionary algorithm," *Information Sciences*, vol. 351, pp. 48–66, 2016.

[31] C. Zhang, W. Lin, D. Ke, and Y. Sun, "Smoothing tie-line power fluctuations for industrial microgrids by demand side control: an output regulation approach," *IEEE Transactions on Power Systems*, vol. 34, no. 5, pp. 3716–3728, 2019.

[32] L. Yang, D. He, and B. Li, "A selection hyper-heuristic algorithm for multiobjective dynamic economic and

environmental load dispatch," *Complexity*, vol. 2020, Article ID 4939268, 2020.

[33] Y. Yang, J. Wu, X. Zhu, and J. Wu, "A hybrid evolutionary algorithm for finding pareto optimal set in multi-objective optimization," in *Proceedings of the Seventh International Conference on Natural Computation (ICNC)*, Shanghai, 2011.

[34] Q. Zhang, H. Li, D. Maringer, and E. Tsang, "MOEA/D with NBI-style tchebycheff approach for portfolio management," in *Proceedings of the IEEE Congress on Evolutionary Computation*, pp. 1–8, Barcelona, Spain, 2010.

[35] R. Shang, Y. Wang, J. Wang, L. Jiao, S. Wang, and L. Qi, "A multi-population cooperative coevolutionary algorithm for multi-objective capacitated arc routing problem," *Information Sciences*, vol. 277, pp. 609–642, 2014.

[36] H. Li and Q. Zhang, "Multi-objective optimization problems with complicated pareto sets, MOEA/D and NSGA-II," *IEEE Transactions on Evolutionary Computation*, vol. 13, no. 2, pp. 284–302, 2009.

[37] A. R. Bhowmik and A. K. Chakraborty, "Solution of optimal power flow using nondominated sorting multi objective gravitational search algorithm," *International Journal of Electrical Power & Energy Systems*, vol. 62, pp. 323–334, 2014.

[38] X. Ma, Q. Zhang, G. Tian, J. Yang, and Z. Zhu, "On tchebycheff decomposition approaches for multiobjective evolutionary optimization," *IEEE Transactions on Evolutionary Computation*, vol. 22, no. 2, pp. 226–244, 2018.

[39] Z. Zhang, Q. Zhang, A. Zhou, M. Gong, and L. Jiao, "Adaptive replacement strategies for MOEA/D," *IEEE Transactions on Cybernetics*, vol. 46, no. 2, pp. 474–486, 2016.

[40] L. Wang, A. Zhou, M. Gong, and L. Jiao, "Constrained subproblems in a decomposition-based multiobjective evolutionary algorithm," *IEEE Transactions on Evolutionary Computation*, vol. 20, no. 3, pp. 475–480, 2016.

[41] G. Yang, Y. Li, Q. Yao, and R. Yong, "Study of reliability of grid connected photovoltaic power based on Monte Carlo method," in *Proceedings of the IEEE Power Engineering and Automation Conference (PEAM)*, pp. 92–95, Wuhan, China, 2011.

[42] H. Hou, M. Xue, Y. Xu et al., "Multiobjective joint economic dispatching of a microgrid with multiple distributed generation," *Energies*, vol. 11, pp. 1–19, 2018.